Stoichiometric and Catalytic Hydroamination of Alkynes and Allene by Zirconium Bisamides $Cp_2Zr(NHR)_2$

Patrick J. Walsh, Anne M. Baranger, and Robert G. Bergman*

Contribution from the Department of Chemistry, University of California, Berkeley, California 94720. *Received July 26, 1991*

Abstract: We have found that the bisamides $Cp_2Zr(NHR)_2$ (**1**) catalyze the hydroamination of alkynes and allene and have investigated the scope and mechanism of this process. Examining both catalytic and stoichiometric additions of 2,6-dimethylaniline to diphenylacetylene in the presence of the corresponding zirconium bisamide **1a** at 95 °C indicates that the reaction is first order in the concentration of bisamide and alkyne and inverse first order in amine. These results are consistent with a reversible rate determining α-elimination of amine and generation of the transient imido complex $Cp_2Zr{=}NR$. Alkyne and amine then compete for this reactive intermediate. While reaction with amine regenerates bisamide, cycloaddition with alkyne provides zirconium azametallacyclobutenes such as **3a**. The metallacycles are rapidly protonated by $ArNH_2$ at the zirconium–carbon bond forming enamide amides (e.g., **6a**) which then undergo α-elimination of enamine to regenerate $Cp_2Zr{=}NAr$ and continue the cycle. Support for the mechanism of the zirconium-catalyzed hydroamination of alkynes (illustrated in Scheme III) was obtained by examining the individual steps of the catalytic reaction in a stoichiometric manner. Several proposed intermediates were independently synthesized and shown to undergo the steps postulated in the catalytic reaction. The ability of bisamides $Cp_2Zr(NHR)_2$ **1a–e** to undergo this process is critically dependent on the size of the zirconium-bound amide ZrNHR. Although all attempts to hydroaminate unstrained or moderately strained olefins have been unsuccessful, hydroamination of the C–C double bond of allene in the presence of **1a** and 2,6-dimethylaniline led to catalytic production of the 2,6-dimethylphenylimine of acetone.

Introduction

The direct addition of organic substrates across unsaturated carbon–carbon bonds is a fundamental process in organic chemistry. An attractive transformation is the addition of an N–H bond across an alkene or alkyne to provide an alkylated amine, enamine, or imine.[1] While this transformation has been realized, it is limited by its lack of generality and regioselectivity.[1a,2] Amines will undergo direct nucleophilic addition to electron-deficient carbon–carbon multiple bonds of perfluoroalkenes[3] or perfluoroalkynes[4] and highly reactive triple bonds such as free benzyne[5] and very strained cycloalkynes.[5,6] However, hydroamination reactions can be assisted or catalyzed by main-group,[1] transition-metal,[7] and lanthanide[8] elements which allow these processes to be performed under milder conditions.

Howk discovered in 1954 that ammonia and primary amines would add to alkenes in the presence of alkali metals or their hydrides, but the reaction typically requires harsh conditions[9a] (175–200 °C, 800–1000 atm). The yields are usually poor, and the reaction gives mono and multiple hydroamination products. More recently Pez and co-workers have reported a more efficient metal–amide-catalyzed addition of diethylamine and ammonia to ethylene and propylene.[9b] Ammonia will add to alkynes at 300–350 °C in the presence of a silica or alumina catalyst, while amines require a zinc or cadmium acetate catalyst.[10] However the most general and practical method for aminating alkenes and alkynes is through the use of Hg^{II} reagents.[11] The conditions employed are mild, and the reaction will tolerate a considerable variety of remote functional groups. The addition of amines to olefins or terminal alkynes in the presence of mercury salts is regiospecific yielding the Markovnikov addition products. In the case of alkynes, enamines are initially formed which isomerize to their tautomeric imines when primary amines are used (eq 1).

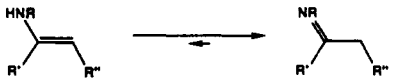

(1)

While aromatic amines cleanly provide the hydroaminated products,[12] reactions with aliphatic amines are complicated by side reactions.[13] Stoichiometric hydroaminations of alkenes and alkynes are most commonly performed using $Hg(OAc)_2$ although methodology has been developed for their catalytic hydroamination using $HgCl_2$.[14] Addition of secondary amines to terminal acetylenes initially gives the enamine derived from Markovnikov addition, but these products isomerize under the reaction conditions to give a mixture of enamine products as shown in eq 2.[14] Catalytic formation of the enamines or imines with primary or secondary aromatic amines in the presence of $Tl(OAc)_3$ has also been observed.[15]

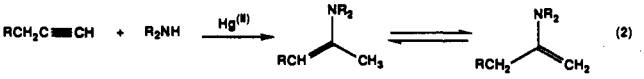

(2)

Transition metals have been used in the hydroamination of olefins to provide Markovnikov addition products.[7] Coordination of olefins to late transition metals activates the olefin toward attack by nucleophiles[16] such as amines[7] to generate σ-alkyl complexes. This process is limited by the ability of the metal to coordinate the olefin. Ethylene as well as monosubstituted and cis- and trans-disubstituted olefins can be used, but other substituted olefins

(1) (a) For a review of additions of amines to alkenes, see: Gasc, M. B.; Latties, A.; Perie, J. J. *Tetrahedron* **1983**, *339*, 703. For a review of addition of amines to alkynes, see: (b) Jäger, V.; Viehe, H. G. *Houben-Weyl, Methoden der Organischen Chemie*; Thieme Verlag: Stuttgart, 1977; Vol. 5/2a, p 713. (c) Chekulaeva, I. A.; Kondrat'eva, L. V. *Russian Chem. Rev.* **1965**, *34*, 669.

(2) March, J. *Advanced Organic Chemistry*; John Wiley & Sons, Inc.: New York, NY, 1985; p 689.

(3) Flowers, W. T.; Haszeldine, R. N.; Owen, C. R.; Thomas, A. *J. Chem. Soc., Chem. Commun.* **1974**, 134.

(4) (a) Le Blanc, M.; Santini, G.; Gallucci, J.; Riess, J. G. *Tetrahedron* **1977**, *33*, 1453. (b) Le Blanc, M.; Santini, G.; Riess, J. G. *Tetrahedron Lett.* **1975**, 4151.

(5) (a) Hoffmann, R. W. In *Chemistry of Acetylenes*; Viehe, H. G., Ed.; Dekker: New York, 1969; p 1063. (b) Hoffmann, R. W. *Dehydrobenzene and Cycloalkynes*; Academic Press: New York, 1967.

(6) Brunet, J. J.; Fixari, B.; Caubere, P. *Tetrahedron* **1974**, *30*, 2931.

(7) Collman, J. P.; Hegedus, L. S.; Norton, J. R.; Finke, R. G. *Principles and Applications of Organotransition Metal Chemistry*; University Science Books: Mill Valley, CA, 1987; Chapters 7.4 and 17.1.

(8) Gagné, M. R.; Marks, T. J. *J. Am. Chem. Soc.* **1989**, *111*, 4108.

(9) (a) Howk, B. W.; Little, E. L.; Scott, S. L.; Whitman, G. M. *J. Am. Chem. Soc.* **1954**, *76*, 1899. (b) Pez, G. P.; Galle, J. E. *Pure Appl. Chem.* **1985**, *12*, 1917.

(10) (a) Miller, S. A. *Acetylene, Its Properties, Manufacture and Uses*; Academic Press: 1965. (b) Kruse, C. W.; Kleinschmidt, R. F. *J. Am. Chem. Soc.* **1961**, *83*, 213. (c) Kruse, C. W.; Kleinschmidt, R. F. *J. Am. Chem. Soc.* **1961**, *83*, 216.

(11) Larock, R. *Angew. Chem., Int. Ed. Engl.* **1978**, *17*, 27.

(12) Barluenga, J.; Azar, F. *Synthesis* **1975**, 704.

(13) Hudrlik, P. F.; Hudrlik, A. *J. Org. Chem.* **1973**, *38*, 4254.

(14) Barluenga, J.; Azar, F.; Liz, R.; Rodes, R. *J. Chem. Soc., Perkin Trans. I* **1980**, 2732.

(15) Barluenga, J.; Azar, F. *Synthesis* **1977**, 195.

(16) (a) Hegedus, L. S. *Tetrahedron* **1984**, *40*, 2415. (b) Åkermark, B.; Bäckvall, J. E.; Zetterberg, K. *Acta Chem. Scand.* **1982**, *B36*, 577.

0002-7863/92/1514-1708$03.00/0 © 1992 American Chemical Society

form very weak complexes with the metal and are subsequently displaced rather than attacked by the amine.

The catalytic hydroamination of olefins in an intermolecular fashion by transition-metal complexes has only been observed with an electron-rich iridium complex. This catalyst is proposed to hydroaminate norbornene via an N–H activation pathway, but only 2–6 turnovers are observed before catalyst decomposition is complete.[17] In contrast to the difficulties encountered with intermolecular hydroamination, the catalytic intramolecular cyclization of amino olefins has been achieved using a variety of catalysts and it provides cyclic amines and enamines.[18] This cyclization reaction works well with aromatic and protected amines (amides, tosylamides, sulfonamides, and ureas).[19] This methodology has been used to synthesize a variety of important classes of nitrogen-containing heterocycles. Recently, Gagné and Marks have designed an intramolecular cyclization of aliphatic amino olefins catalyzed by organolanthanocene complexes. The reaction is highly regiospecific furnishing five- and six-membered cyclic amines under mild conditions.[8]

Due to the difficulties associated with hydroamination reactions and our interest in the application of metal–ligand multiply bonded species[20] to organic transformations we have investigated the possibility of carrying out hydroamination reactions catalyzed by zirconocene bisamides $Cp_2Zr(NHR)_2$. We have found that such reactions work well with alkynes and allene, leading to enamines and imines. In this paper we report the synthesis and characterization of the zirconocene bisamides and alkyl amides, and the enamine and imine products isolated from the hydroamination of alkynes. We also present kinetic evidence which supports the intermediacy of the imido complex $Cp_2Zr{=}NR$ and its alkyne cycloaddition product, the azametallacyclobutene, in the zirconium-catalyzed reactions with alkynes.[21]

Results

Synthesis of Bisamides $Cp_2Zr(NHR)_2$ and Alkyl Amides $Cp_2Zr(NHR)(R')$. Lithium amides have been shown to react with early transition-metal chlorides to provide metal amides in high yield.[22] This methodology is useful in the synthesis of the bisamides $Cp_2Zr(NHR)_2$ (**1a–c**; eq 3).[23] A complementary route

$$Cp_2ZrCl_2 + 2\,LiNHR \xrightarrow[25\ ^\circ C]{THF} \underset{\mathbf{1}}{Cp_2Zr(NHR)_2} + 2\,LiCl \qquad (3)$$

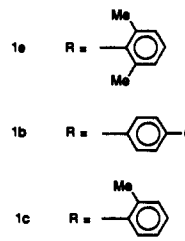

to the bisamides **1a**, **1b**, **1d**, and **1e** involved thermolysis of Cp_2ZrMe_2[24] in toluene with 4 equiv of amine (Scheme I). When

Scheme I

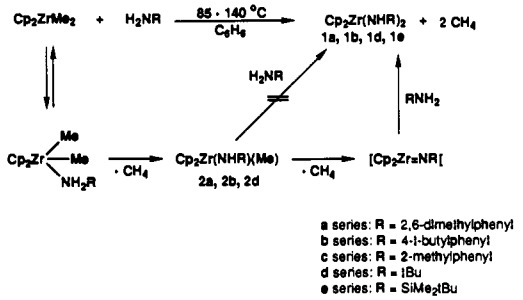

the reactions were conducted in sealed NMR tubes in C_6D_6, methane was identified by ^1H NMR (δ 0.15 ppm). The alkyl amides $Cp_2Zr(NHR)(R')$ (**2a**, R = 2,6-dimethylphenyl, R′ = Me; **2b**, R = 4-*tert*-butylphenyl, R′ = Me; **2c**, R = 2-methylphenyl, R′ = 3,3-dimethylbutyl; **2d**, R = *tert*-butyl, R′ = Me; **2e**, R = *tert*-butyldimethylsilyl, R′ = $CH_2CH_2CMe_3$) have been synthesized by the addition of lithium amide LiNHR to the alkyl chlorides $Cp_2Zr(R')(Cl)$ (R′ = Me, $CH_2CH_2CMe_3$) (eq 4). Several of these materials (compounds **1a–e** and **2b–e**) were prepared in the course of a companion study,[25] and the remainder are described here (see Experimental Section).

$$Cp_2Zr(R')(Cl) + LiNHR \xrightarrow[25\ ^\circ C]{THF} Cp_2Zr(NHR)(R') + LiCl \qquad (4)$$

Product	R	R′
2e	2,6-dimethylphenyl	Me
2b	4-*tert*-butylphenyl	Me
2c	2-methylphenyl	$CH_2CH_2CMe_3$
2d	*tert*-butyl	Me
2e	*tert*-butyldimethylsilyl	$CH_2CH_2CMe_3$

Heating the methyl amides **2a**, **2b**, and **2d** to 85 °C with the corresponding amine provided the bisamides **1a**, **1b**, and **1d** all in >95% yield (^1H NMR) (Scheme I). Heating alkyl amide **2b** in the presence of 1.87, 3.97, and 5.58 equiv of 4-*tert*-butylaniline and monitoring the rates of reaction by ^1H NMR spectrometry gave rate constants of 4.97, 5.10, and 4.76 × 10^{-5} s^{-1}, respectively, which indicated the reaction was cleanly first order in **2b** and independent of the concentration of amine. In the case of the bisamides **1d** and **1e** the synthesis from Cp_2ZrMe_2 and the corresponding amine was the method of choice; the reaction of the lithium amides with zirconocene dichloride led only to intractable products.

Formation of Azametallacyclobutenes. Thermolysis of certain bisamides **1** in the presence of selected internal alkynes in benzene between 85 and 120 °C resulted in a dramatic change in the color of the solution from pale yellow to intensely colored due to the formation of the cycloaddition products, the azametallacyclobutenes **3** and **4** (eq 5). However, some of the bisamides will

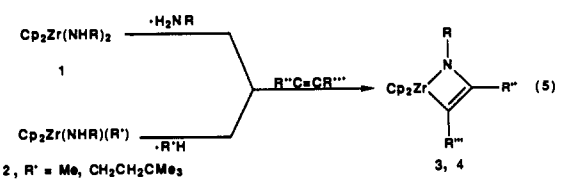

(5)

Product	R	R″
3e	2,6-dimethylphenyl	Ph
3e	Si(*t*-Bu)Me_2	Ph
4e	2,6-dimethylphenyl	*p*-tol

not undergo this elimination–cycloaddition sequence; for example, thermolysis of the bisamide **1e** with diphenylacetylene at 140 °C resulted in no reaction after 6 days. We have also found the formation of the metallacycle to be reversible (eq 6). Heating the azametallacyclobutene **3a** to 45 °C in the presence of 5.0 equiv

(17) Casalnuovo, A. L.; Calabrese, J. C.; Milstein, D. *J. Am. Chem. Soc.* **1988**, *110*, 6738.
(18) Hegedus, L. S. *Angew. Chem., Int. Ed. Engl.* **1988**, *27*, 1113.
(19) Tamaru, Y.; Hojo, M.; Higashimura, H.; Yoshida, Z. *J. Am. Chem. Soc.* **1988**, *110*, 3994.
(20) Nugent, W. A.; Mayer, J. M. *Metal–Ligand Multiple Bonds*; John Wiley & Sons: New York, 1988.
(21) Portions of this work have been communicated: (a) Walsh, P. J.; Hollander, F. J.; Bergman, R. G. *J. Am. Chem. Soc.* **1988**, *110*, 8729. For closely related work, see: (b) Cummins, C. C.; Baxter, S. M.; Wolczanski, P. T. *J. Am. Chem. Soc.* **1988**, *110*, 8731. (c) Cummins, C. C.; Schaller, C. P.; Van Duyne, G. D.; Wolczanski, P. T.; Chan, A. W. E.; Hoffmann, R. *J. Am. Chem. Soc.* **1991**, *113*, 2985.
(22) Lappert, M. F.; Power, P. P.; Sanger, A. R.; Srivastava, R. C. *Metal and Metalloid Amides*; John Wiley & Sons: New York, 1980.
(23) Throughout this paper compounds have been assigned letters based on the organic moiety attached to nitrogen. For example, all compounds that containing an **a** are substituted with the *N*-2,6-dimethylphenyl group. Similarly compounds numbers followed by **b** use the 4-*tert*-butylphenyl substituent, etc.
(24) Wailes, P. C.; Weigold, H.; Bell, A. P. *J. Organomet. Chem.* **1972**, *34*, 155.
(25) Walsh, P. J.; Bergman, R. G., manuscript in preparation.

Table I. Crystal and Data Collection Parameters[a]

	3a	7a
temp (°C)	25	−114
empirical formula	$C_{32}H_{29}NZr$	$C_{22}H_{21}N$
formula wt (amu)	518.8	299.4
crystal size (mm)	0.17 × 0.38 × 0.38	0.18 × 0.40 × 0.50
space group	$P2_1/c$	$P\bar{1}$
a (Å)	22.7892 (19)	8.819 (3)
b (Å)	12.3324 (23)	8.930 (2)
c (Å)	19.3120 (18)	11.466 (2)
α (°)	90.0	98.24 (2)
β (°)	110.387 (8)	90.55 (2)
γ (°)	90.0	109.92 (2)
V (Å^3)	5078.6 (21)	839.6 (8)
Z	8	2
d_{calc} (gcm^{-3})	1.35	1.19
μ_{calc} (cm^{-1})	4.4	0.6
reflcns measd	$\pm h,+k,+l$	$+h,\pm k,\pm l$
scan width	$\Delta\theta = 0.65 + 0.35 \tan\theta$	$\Delta\theta = 0.65 + 0.35 \tan\theta$
scan speed (θ, deg/m)	0.97 → 6.70	6.70
setting angles (2θ, deg)[b]	28–28	22–28
vert aperture (mm)	3.0	4.0
horiz aperture (mm)	2.2 + 1.0 tan θ	2.0 + 1.0 tan θ

[a] Parameters common to all structures: radiation, Mo Kα (λ = 0.71073 Å); monochromator, highly oriented graphite ($2\theta_m$ = 12.2°); detector: crystal scintillation counter, with PHA; 2θ range, 3 → 45°; background, measured over 0.25 ($\Delta\theta$) added to each end of the scan; intensity standards, measured every hour of X-ray exposure time; orientation, three reflections were checked after every 200 measurements. Crystal orientation was redetermined if any of the reflections were offset from their predicted positions by more than 0.1°. [b] Unit cell parameters and their esd's were derived by a least-squares fit to the setting angles of the unresolved Mo Kα components of 24 reflections with the given 2θ range. In this and all subsequent tables the esd's of all parameters are given in parentheses, right-justified to the least significant digit(s) of the reported value.

of di-*p*-tolylacetylene for 4 days resulted in the establishment of an equilibrium between the azametallacyclobutenes **3a** and **4a** and the free alkynes as determined by ^{1}H NMR spectrometry.

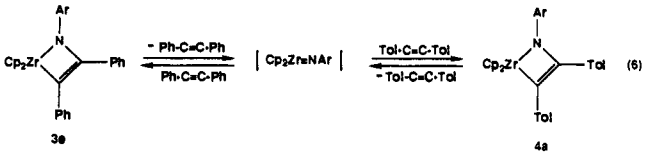

X-ray Diffraction Study of Azametallacyclobutene 3a. The ^{1}H and ^{13}C{^{1}H} NMR spectra of the azametallacyclobutenes each contain only one resonance for the cyclopentadienyl ligands indicating that the cyclopentadienyl rings are equivalent on the NMR time scale and the metallacycle is either planar or rapidly undergoing ring inversion. The connectivity of the metallacycles was confirmed in the case of the cycloaddition product of $Cp_2Zr{=}NR$ (R = 2,6-dimethylphenyl) with diphenylacetylene, **3a**, by an X-ray crystallographic study. Brown prismatic crystals were obtained by liquid diffusion of hexanes into a solution of **3a** in toluene at −30 °C. X-ray data on a single crystal were collected at 25 °C under conditions summarized in Table I. The structure was solved by Patterson methods and refined by standard Fourier techniques. Structural refinement is described in the Experimental Section; positional parameters and structure factors are provided as supplementary material. Relevant bond distances, bond angles, and torsional angles are listed in Tables II, III, and IV. The molecule crystallizes in the space group $P2_1/c$ with two independent molecules in the asymmetric unit cell. These molecules are chemically identical but crystallographically nonequivalent, showing small conformational differences which are best seen by comparison of the torsional angles and the least squared planes. The bond distances and angles of the two asymmetric molecules are nearly identical (Tables II and III). The ORTEP diagram shown in Figure 1 illustrates the near planarity of the metallacycle. The average Zr–N and Zr–C bond lengths of the two asymmetric

Table II. Selected Intramolecular Distances and esd's for Molecule 1 of Complex **3a** and for Complex **7a**

compd	atom 1	atom 2	distance
3a	Zr1	N1	2.093 (3)
	Zr1	C11	2.532 (5)
	Zr1	C12	2.203 (3)
	Zr1	CP1	2.244
	Zr1	CP2	2.222
	N1	C11	1.426 (5)
	N1	C13	1.413 (6)
	C11	C12	1.361 (8)
	C11	C21	1.487 (7)
	C12	C27	1.463 (6)
7a	N1	C1	1.398 (4)
	N1	C15	1.426 (4)
	C1	C2	1.357 (4)
	C1	C9	1.488 (4)
	C2	C3	1.485 (4)

Table III. Selected Intramolecular and Torsional Angles for Molecule 1 of Complex **3a** and for Complex **7a**

compd	atom 1	atom 2	atom 3	atom 4	angle
3a	N1	Zr1	C12		66.33 (12)
	N1	Zr1	CP1		120.2
	N1	Zr1	CP2		107.0
	C12	Zr1	CP1		103.5
	C12	Zr1	CP2		114.2
	CP1	Zr1	CP2		128.3
	Zr1	N1	C11		90.0 (3)
	Zr1	N1	C13		140.8 (2)
	C11	N1	C13		122.6 (4)
	N1	C11	C12		115.1 (4)
	N1	C11	C21		117.9 (5)
	C12	C11	C21		126.4 (4)
	Zr1	C12	C11		87.2 (2)
	Zr1	C12	C27		139.9 (3)
	C11	C12	C27		128.0 (4)
	N1	C13	C14		123.1 (5)
	N1	C13	C18		117.5 (5)
	C12	Zr1	N1	C11	6.87 (0.23)
	N1	Zr1	C12	C11	−7.21 (0.25)
	Zr1	N1	C11	C12	−11.31 (0.38)
7a	C1	N1	C15		124.1 (3)
	C2	C1	N1		122.4 (3)
	C9	C1	N1		111.2 (3)
	C2	C1	C9		126.3 (3)
	C1	C2	C3		126.8 (3)

molecules are 2.102 (2) Å and 2.208 (3) Å, and the C11–C12 bond length of 1.366 (6) Å is clearly a double bond.

In a related investigation we have synthesized the monomeric imido complex $Cp_2Zr(=NAr)(THF)$ (**5a**, Ar = 2,6-dimethylphenyl) in a manner analogous to that reported for the *tert*-butyl imido complex $Cp_2Zr(=NCMe_3)(THF)$.[21] Because THF dissociates rapidly and reversibly from the zirconium center, these complexes are a convenient source of the reactive intermediate $Cp_2Zr{=}NAr$ at temperatures lower than that needed to generate the imido intermediate from either the alkyl amides or the bisamides (85–120 °C). Alkynes react rapidly with the THF adduct at room temperature to form the corresponding azametallacyclobutenes (eq 7). For example, when diphenylacetylene was added to $Cp_2Zr(=NAr)(THF)$ the solution turned from pale yellow to the brown of **3a** within seconds. The yield was determined to be 97% by ^{1}H NMR integration against an internal standard.

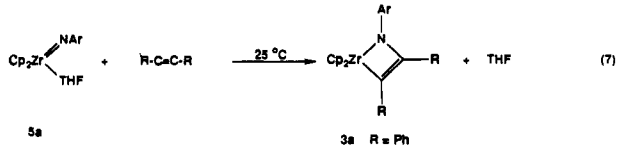

Reactions of Azametallacycles with Amine. Most of the metallacycles can be protonated with additional amine leading to enamine and regenerating the bisamide. For example, metallacycle

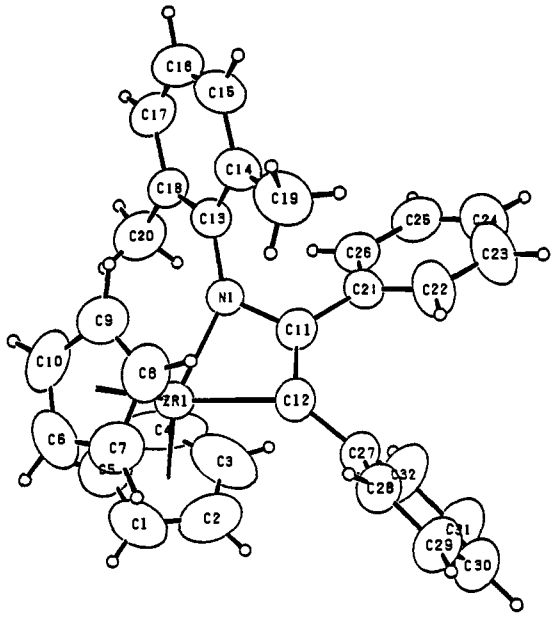

Figure 1. Geometry and labeling scheme for molecule 1 of **3a**. The ellipsoids are scaled to represent the 50% probability surface. Hydrogen atoms are given as arbitrarily small spheres for clarity.

Scheme II

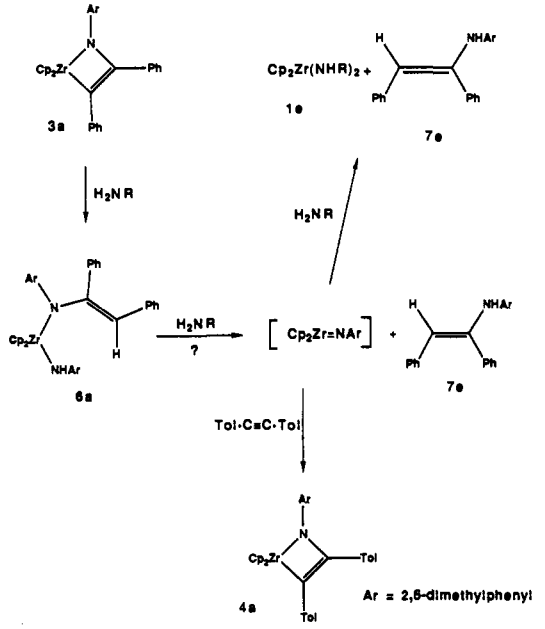

3a reacted with 2 equiv of 2,6-dimethylaniline at 45 °C over 40 h to form the bisamide **1a** and enamine **7a** each in 97% yield as determined by ^1H NMR and illustrated in Scheme II. However, an exception to this behavior was observed with metallacycle **3e**. Heating the metallacycle with 2.2 equiv of *tert*-butyldimethylsilylamine at 95 °C for 4 days resulted in regeneration of diphenylacetylene along with an equivalent of bisamide **1e** as shown in eq 8. This reaction also takes place at 45 °C although at that temperature it requires several weeks.

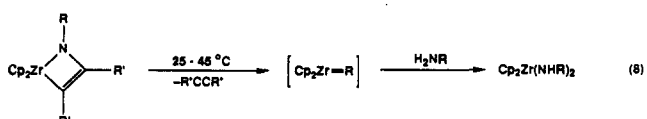

3e R = Si(t-Bu)Me2, R' = Ph

When complex **3a** was treated with 1 rather than 2 equiv of 2,6-dimethylaniline, the color of the solution changed from brown to yellow over a 15-min period with formation of a new complex

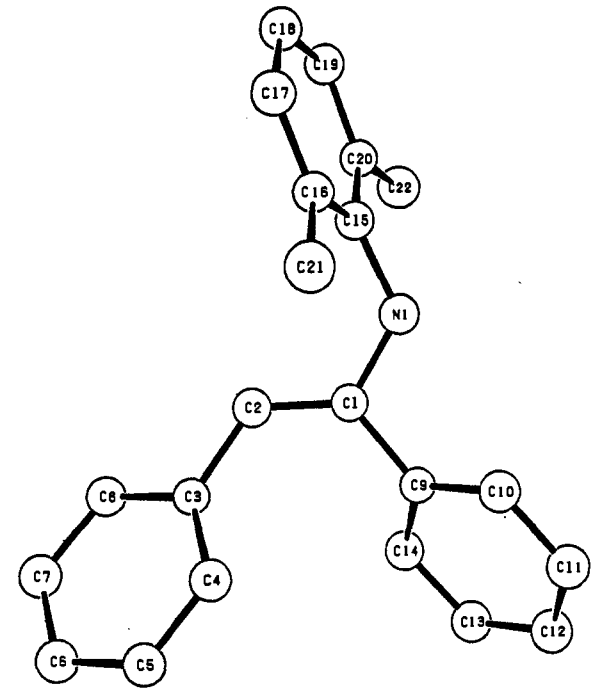

Figure 2. Geometry and labeling scheme for **7a**. The ellipsoids are scaled to represent the 50% probability surface.

6a (Scheme II) which was isolated in 67% yield after recrystallization from toluene layered with hexanes at −30 °C. The ^1H and $^{13}C\{^1H\}$ NMR spectra of **6a** at 25 °C contain broad resonances (presumably due to hindered rotation). However the low temperature ^1H and $^{13}C\{^1H\}$ NMR are sharp and consistent with the N-bound enamide amide structure shown in Scheme II which arises via protonation of the Zr–C bond of the azametallacyclobutene by 2,6-dimethylaniline. The $^{13}C\{^1H\}$ NMR is especially informative in assigning the regiochemistry of the protonation of **3a**. Resonances for sp^2 hybridized carbons bound to the Cp_2Zr fragment typically fall between 170 and 190 ppm in the $^{13}C\{^1H\}$ NMR.[26] Complex **6a** exhibits no resonances downfield of 157 ppm in the $^{13}C\{^1H\}$ NMR. Further support for the proposed structure was gained by IR spectrometry. The IR spectrum of **6a** (C_6H_6) exhibits an N–H stretch at 3296 cm^{-1}. The enamide amide **6a** reacted cleanly with 2,6-dimethylaniline at 45 °C over an 8-h period to form the bisamide **1a** in 97% yield (^1H NMR) as illustrated in Scheme II. Enamide amide **6a** also reacted with di-*p*-tolylacetylene at 45 °C over an 8-h period to form the metallacycle **4a** in >98% yield (Scheme II) as determined by ^1H NMR integration against an internal standard. The low temperature required for generation of $Cp_2Zr{=}NAr$ (45 °C vs 85 °C for elimination of amine from bisamide **1a**) and the product observed in this reaction (**4a**) indicate that **6a** undergoes α-elimination of enamine to generate the imido complex $Cp_2Zr{=}NAr$.

Zirconium-Catalyzed Conversion of Alkynes and Amines to Enamines. When a catalytic amount (3 mol %) of the bisamide **1a** or **1d** was heated to 95–120 °C in the presence of the corresponding amine and 2-butyne or diphenylacetylene, enamines were catalytically formed (eq 9).[27] Under the reaction conditions the

(26) For example, the ^{13}C resonances for the corresponding sp^2 hybridized carbon in $Cp^*_2ZrPh_2$ is 193.5 ppm. See: (a) Schock, L. E.; Brock, C. P.; Marks, T. J. *Organometallics* **1987**, *6*, 232. In the metallacycle $Cp_2Zr(CPhCPhCHNSiMe_3)$ the sp^2 hybridized carbon bound to Zr resonates at 187.0 ppm, see: (b) Buchwald, S. L.; Wannamaker, M. W.; Watson, B. T. *J. Am. Chem. Soc.* **1989**, *111*, 776. Buchwald, S. L.; Watson, B. T.; Wannamaker, M. W.; Dewan, J. C. *J. Am. Chem. Soc.* **1989**, *111*, 4486.

Table IV. Initial Concentrations and Rate Constants[a] for the Catalytic Hydroamination of Diphenylacetylene in the Presence of 2,6-Dimethylaniline and **1a**

expt no.	$[amine]_0$ (M)	[**1a**] (M)	[alkyne] (M)	k_{obs} (M^2 s^{-1})	k_1k_2/k_{-1} (s^{-1})
1	0.0172	2.57×10^{-3}	0.174	5.54×10^{-9}	1.24×10^{-5}
2	0.0183	3.57×10^{-4}	0.175	1.00×10^{-9}	1.60×10^{-5}
3	0.0187	1.18×10^{-3}	0.200	3.18×10^{-9}	1.35×10^{-5}
4	0.0171	5.60×10^{-3}	0.164	1.17×10^{-8}	1.27×10^{-5}
5	0.0176	2.33×10^{-3}	0.238	8.17×10^{-9}	1.47×10^{-5}
6	0.0169	2.41×10^{-3}	0.316	9.02×10^{-9}	1.18×10^{-5}
7	0.0175	2.40×10^{-3}	0.405	1.22×10^{-9}	1.25×10^{-5}

[a] Standard deviation in measured k_{obs} values:±2%. Error in overall determination of k_1k_2/k_{-1}:±10%.

enamine formed from 2-butyne was observed by ^1H NMR but tautomerized to its isomeric imine, whereas **7a** was isolated as the enamine and characterized by X-ray crystallography which confirmed the cis nature of the phenyl groups. Data collection parameters from the X-ray diffraction study of **7a** are given in Table I with selected bond lengths and bond angles in Tables II and III. An ORTEP diagram is shown in Figure 2. Although the enamine **7a** is isolated, this isomer is not the thermodynamic product: addition of I_2 in light to **7a** catalyzed its conversion to the imine (eq 10). However, we did not observe the isomer of **7a** with trans phenyl groups and cannot rule out its formation followed by isomerization to **7a** under the reaction conditions. In a control experiment, 2,6-dimethylaniline was heated to 120 °C with diphenylacetylene in the absence of catalyst for 3 days during which no reaction was observed.

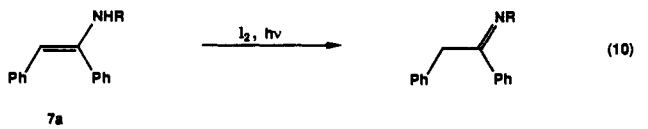

(10)

7a

At 110 °C, the catalytic formation of enamine with 3 mol % of the catalyst and 30 equiv each of the amine and alkyne was relatively slow. For example, hydroamination of 2-butyne with catalyst **1a** occurred with a rate of 0.04 turnovers/h at 110 °C; the same catalyst gave 0.2 turnovers/h with diphenylacetylene. However, the catalyst seems to be indefinitely stable to the reaction conditions. In cases with less reactive bisamides or sterically hindered alkynes catalytic hydroamination is not observed. For example thermolysis of the bisamide **1d** in the presence of 2-butyne at 140 °C resulted in no reaction. Similarly, heating the more reactive bisamide **1a** with 4,4-dimethyl-2-pentyne produced no enamine after several weeks at 110 °C.

The proposed mechanism for the catalytic hydroamination is shown in Scheme III. To test this mechanism, kinetic studies were performed on the catalytic formation of enamine **7a** from diphenylacetylene and 2,6-dimethylaniline at 95 °C using the bisamide **1a** as the catalyst. In order to minimize inhibition by amine (see below), reactions were run using excess alkyne (to keep its concentration effectively constant) and the rate followed by monitoring the disappearance of $ArNH_2$ by ^1H NMR integration against an internal standard. The reactions were followed until >98% conversion to the enamine was observed. The conditions for the kinetic experiment are described in the Experimental Section; the concentrations of 2,6-dimethylaniline, diphenylacetylene, and the bisamide catalyst **1a** are listed in Table IV. The concentration ranges used were limited somewhat in order to maximize the accuracy of the data that we were able to collect using the NMR technique.

NMR analysis also showed that the catalyst was stable and that its concentration remained constant. However, the integrated initial concentrations of catalyst were consistently lower than those calculated by weight, and trace cyclopentadienyl containing contaminants were detected by ^1H NMR spectrometry. This initial decomposition was presumably due to traces of water on the glassware. Attempts to remedy this situation, including silylating the NMR tubes, were not successful, and so the concentration of the catalyst was determined by ^1H NMR integration against an internal standard. Plots of $[amine]^2/2$ vs time gave straight lines consistent with the reaction being inverse first order in the amine (see Discussion section). Typical plots for the dependence of [amine] vs time and $[amine]^2/2$ vs time are given in Figures 3 and 4, respectively. Plots of k_{obs} vs the concentration of the alkyne or the catalyst yielded straight lines as illustrated in Figures 5 and 6. In this way the reaction was also found to be first order in these components. The overall experimental rate law is summarized in eq 11.

$$\text{Rate} = k_{obs}\frac{[RC{\equiv}CR]\,[Cp_2Zr(NHR)_2]}{[RNH_2]} \qquad (11)$$

Reactions of Olefins with Amines in the Presence of Bisamide Catalysts. We have been unable to extend the alkyne hydroamination to unstrained or even mildly strained alkenes. For example, when bisamide **1d** was heated with norbornene for 28 h at 155 °C, no reaction was observed. Similarly, when bisamide **1a** was heated for 24 h at 135 °C with 5 atm of ethylene and 10 equiv of 2,6-dimethylaniline or for 24 h at 160 °C in the presence of 12 equiv each of allylbenzene and 2,6-dimethylaniline, no addition of amine to the olefin occurred. However the more reactive double bond of allene was hydroaminated catalytically by the bisamide **1a** at 90 °C (eq 12). The anti-Markovnikov addition product, the 2,6-dimethylphenylimine of acetone (**8**), was isolated in 83% yield. This material was identified by independent synthesis from acetone and 2,6-dimethylaniline and by its spectroscopic properties, which included a strong absorption in the IR spectrum at 1694 cm^{-1} assigned to the C=N stretch.

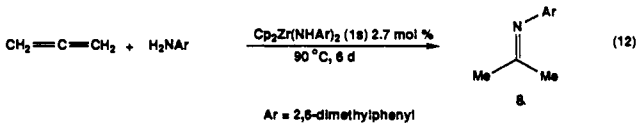

(12)

8

Ar = 2,6-dimethylphenyl

Discussion

Stoichiometric Reactions of $Cp_2Zr{=}NR$ with Alkynes. In analogy to the α-elimination of methane from the methyl amides, heating bisamides **1a** and **1d** results in reversible α-elimination of amine from the bisamide to generate the transient imido complex $Cp_2Zr{=}NR$. The intermediate $Cp_2Zr{=}NR$ can, however, be trapped with internal alkynes to provide azametallacyclobutenes (eq 5). The reversible α-elimination of amine from a stable bisamide is uncommon but has been observed.[28-30] A similar cycloaddition of alkylidenes with alkynes to yield metallacyclobutenes has been reported,[31] and these metallacycles have

(27) The catalytic hydroamination of unsymmetrical alkynes can also be performed with this system. These reactions will be discussed in a separate paper concerned with the regiochemistry of the hydroamination reaction.

(28) Profilet, R. D.; Zambrano, C. H.; Fanwick, P. E.; Nash, J. J.; Rothwell, I. P. *Inorg. Chem.* **1990**, *29*, 4364.

(29) Chan, D. M.-T.; Fultz, W. C.; Nugent, W. A.; Roe, D. C.; Tulip, T. H. *J. Am. Chem. Soc.* **1985**, *107*, 251.

(30) Hill, J. E.; Profilet, R. D.; Fanwick, P. E.; Rothwell, I. P. *Angew. Chem., Int. Ed. Engl.* **1990**, *29*, 664.

(31) (a) Brown-Wensley, K. A.; Buchwald, S. L.; Cannizzo, L.; Clawson, L.; Ho, S.; Meinhardt, D.; Stille, J. R.; Straus, D.; Grubbs, R. H. *Pure Appl. Chem.* **1983**, *55*, 1733. (b) Tebbe, F. N.; Harlow, R. L. *J. Am. Chem. Soc.* **1980**, *102*, 3210. (c) McKinney, R. J.; Tulip, T. H.; Thorn, D. L.; Coolbaugh, T. S.; Tebbe, F. N. *J. Am. Chem. Soc.* **1981**, *103*, 5584. (d) Wood, C. D.; McLain, S. J.; Schrock, R. R. *J. Am. Chem. Soc.* **1979**, *101*, 3210. (e) Mayr, A.; Lee, K. S.; Kjelsberg, M. A.; Van Engen, D. *J. Am. Chem. Soc.* **1986**, *108*, 6079.

been proposed as intermediates in the polymerization of acetylenes.[32] When a heteroatom is multiply bonded to the metal center, the cycloaddition reactions are rare. It is likely that an azametallacyclobutene is an intermediate in the double insertion of dimethylacetylenedicarboxylate into the iridium imido complex Cp*Ir=N-*t*-Bu to furnish the η^4-pyrrole (eq 13)[33] and that an

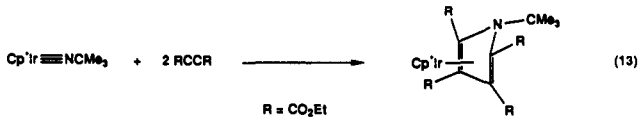

oxametallacycle is an intermediate in the triphenylphosphine induced alkyne cycloaddition of Cp^*ReO_3 to provide a metallapyran (eq 14).[34] Sharpless and co-workers have proposed that

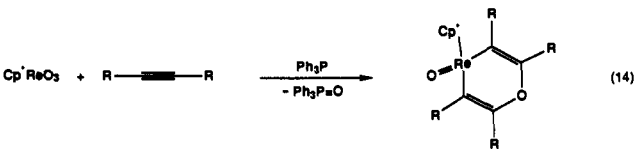

the reaction of OsO_4 with olefins proceeds by an initial [2 + 2] cycloaddition to give an intermediate oxametallacyclobutane which rearranges to the isolable five-membered ring osmate ester (eq 15).[35] We have also found that the bis(pentamethylcyclo-

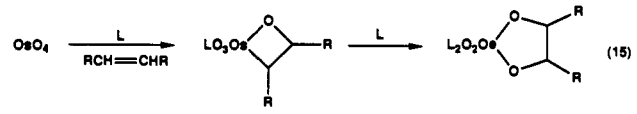

pentadienyl)zirconium oxo and sulfido intermediates $Cp^*_2Zr{=}O$ and $Cp^*_2Zr{=}S$ react cleanly with internal alkynes to furnish oxa- and sulfametallacyclobutenes (eqs 16 and 17).[36]

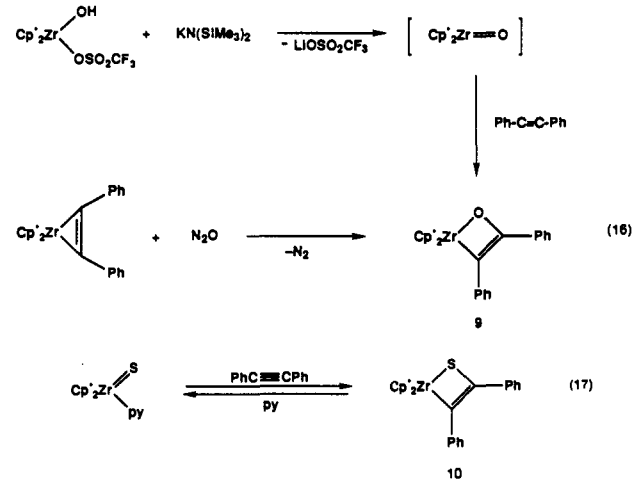

The structure of **3a** (Figure 1) is similar to the bis(pentamethylcyclopentadienyl)zirconium heterometallacyclobutenes containing oxygen (**9**) and sulfur (**10**). Hillhouse and co-workers recently synthesized the oxametallacyclobutene **9** by the oxidation of the diphenylacetylene adduct $Cp^*_2Zr(C_2Ph_2)$ with N_2O as shown in eq 16.[37] The Zr–O, Zr–C, and C–C bond lengths of

Scheme III

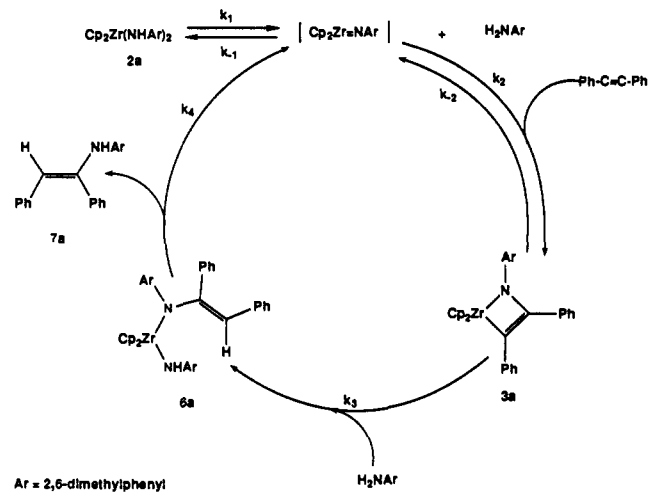

the metallacycle **9** (2.065 (5), 2.219 (7), and 1.348 (12) Å, respectively) compare closely to the Zr–N, Zr–C, C–C of **3a** (2.103 (3), 2.208 (3), and 1.366 (6)) (note that these distances are average values for the two molecules in the unit cell). The sulfur analogue **10** was synthesized in our labs by the cycloaddition of diphenylacetylene with the monomeric sulfido complex $Cp^*_2Zr(=S)(py)$ (eq 17) at 85 °C.[36] The Zr–S, Zr–C, and the C–C bond distances of the sulfametallacycle are 2.505 (1), 2.226 (4), and 1.330 (6) Å, respectively.

Azametallacyclobutene **3a** and di-*p*-tolylacetylene equilibrate thermally (45 °C) to an equilibrium mixture of the metallacycles **3a** and **4a** (eq 6). Alkyne exchange presumably occurs via a cycloreversion liberating free alkyne and the imido intermediate $Cp_2Zr{=}NR$, which is then trapped by one of the diarylacetylenes. Similar cycloreversions have been observed[38] with the titanacyclobutenes. When titanacyclobutenes incorporating bulky internal acetylenes are heated, cycloreversion takes place readily to generate a reactive titanocene methylidene complex.[39] The permethylzirconocene oxa- and sulfametallocyclobutenes also exhibit reversible cycloaddition chemistry. In the case of the sulfametallacyclobutene **10** the proposed intermediate sulfido complex $Cp^*_2Zr{=}S$ can be trapped by substituted pyridines to afford the pyridine adduct $Cp^*_2Zr(=S)(L)$ and the free alkyne (eq 17).[36]

The Zirconium-Catalyzed Addition of Amines to Alkynes. When amines and internal alkynes were heated in the presence of a small amount of the bisamide catalysts **1a** or **1d** at 95–120 °C, enamines (or their imine isomers) were formed catalytically as illustrated in Scheme III. The imine/enamine equilibrium is slowest in the case of **7a** because the enamine is highly conjugated.[40] In the formation of **7a** only the isomer with the phenyl rings cis was formed as established by an X-ray diffraction study; an ORTEP diagram is shown in Figure 2. The bond angles and bond lengths (Tables II and III, respectively) are similar to those of structurally characterized enamines.[41]

As discussed in the Results section, the rates of the catalytic hydroamination using various alkyne and catalyst concentrations are listed in Table IV. The proposed mechanism for the catalytic cycle is depicted in Scheme III. Upon thermolysis of the bisamide complex **1a** we propose that rate-determining α-elimination of amine occurs to form the transient imido complex $Cp_2Zr{=}NAr$ (Ar = 2,6-dimethylphenyl). The amine and alkyne then compete for the reactive imido intermediate. Trapping of this intermediate

(32) (a) Masuda, T.; Susaki, N.; Higashimura, T. *Macromolecules* **1975**, *8*, 717. (b) Katz, T. J.; Hacker, S. M.; Kendrick, R. D.; Yannoni, C. S. *J. Am. Chem. Soc.* **1985**, *107*, 2182. (c) Strutz, H.; Dewan, J. C.; Schrock, R. R. *J. Am. Chem. Soc.* **1985**, *107*, 5999. (d) Ivin, K. J.; Rooney, J. J.; Stewart, C. D.; Green, M. L. H. *J. Chem. Soc., Chem. Commun.* **1978**, 604.

(33) Glueck, D. S.; Hollander, F. J.; Bergman, R. G. *J. Am. Chem. Soc.* **1989**, *111*, 2719.

(34) DeBoer, E. J. M.; Dewith, J.; Orpen, A. G. *J. Am. Chem. Soc.* **1986**, *108*, 8271.

(35) (a) Sharpless, K. B.; Teranishi, A. Y.; Blackvall, J.-E. *J. Am. Chem. Soc.* **1977**, *99*, 3120. (b) Hentges, S. G.; Sharpless, K. B. *J. Am. Chem. Soc.* **1980**, *102*, 4263.

(36) Carney, M. J.; Walsh, P. J.; Hollander, F. J.; Bergman, R. G. *J. Am. Chem. Soc.* **1990**, *112*, 6426.

(37) Vaughan, G. A.; Sofield, C. D.; Hillhouse, G. L.; Rheingold, A. L. *J. Am. Chem. Soc.* **1989**, *111*, 5491.

(38) McKinney, R. J.; Tulip, T. H.; Thorn, D. L.; Coolbaugh, T. S.; Tebbe, F. N. *J. Am. Chem. Soc.* **1981**, *103*, 5584.

(39) Brown-Wensley, K. A.; Buchwald, S. L.; Cannizzo, L.; Clawson, L.; Ho, S.; Meinhardt, D.; Stille, J. R.; Straus, D.; Grubbs, R. H. *Pure Appl. Chem.* **1983**, *55*, 1733.

(40) Shainyan, B. A.; Mirskova, A. N. *Russian Chem. Rev.* **1979**, *48*, 107.

(41) Cook, A. G. *Enamines: Synthesis, Structure, and Reactions*; Marcel Dekker, Inc.: New York, NY, 1988.

with amine (k_{-1}) regenerates the starting bisamide complex, and therefore excess amine is predicted to inhibit the reaction while cycloaddition of the alkyne with the imido complex (k_2) gives the azametallacyclobutene. The azametallacyclobutene can also undergo retrocyclization to liberate the alkyne and generate the imido intermediate via the k_{-2} path. Alternatively, the metallacycle can react with amine through k_3 leading to the enamine and $Cp_2Zr{=}NR$, beginning the catalytic cycle again.

Although $Cp_2Zr{=}NAr$ and metallacycle **3a** are proposed as intermediates, neither of these two species were observed in the catalytic reaction. However several steps in the catalytic cycle which support their intermediacy were established by study of appropriate stoichiometric reactions. We have already discussed in detail reactions in which $Cp_2Zr{=}NR$, generated as a transient species, leads to isolable metallacycles. As a closer model for the k_2 step in the catalytic cycle, we examined the reaction of the THF adduct of the monomeric imido complex $Cp_2Zr(=NAr)(THF)$ (**5a**) with diphenylacetylene. Upon addition of diphenylacetylene to **5a** at room temperature the solution immediately turned brown, the color of the metallacycle **3a** in solution. Formation of **3a** was confirmed by ^1H NMR spectrometry and integration against an internal standard, which indicated that the reaction proceeded in 97% yield. The rate of reaction of $Cp_2Zr{=}NAr$ with alkyne in the catalytic cycle is expected to be at least as fast as that of the THF adduct **5a** because the intermediate does not need to dissociate ligand as **5a** does.

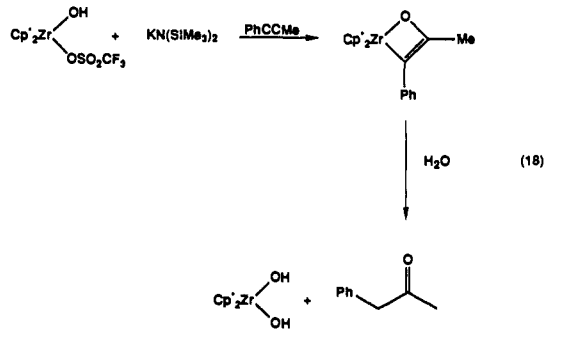

Using independently synthesized **3a** the k_{-2} and k_3 steps were more closely examined. The k_{-2} step represents the cycloreversion of the metallacycle **3a** to liberate diphenylacetylene and generate the imido intermediate. Heating the metallacycle **3a** to 45 °C with 5 equiv of di-*p*-tolylacetylene for 4 days established an equilibrium between the metallacycles **3a** and **4a** and free alkynes (eq 6). The k_3 step of the cycle was established by showing that 1 equiv of 2,6-dimethylaniline reacts with metallacycle **3a** in benzene at 25 °C in 15 min to give the monoprotonated intermediate **6a**, the enamide amide (Scheme II).

The isolation of enamide amide **6a** allowed us to examine the last step in the catalytic cycle outlined in Scheme III. Two possible mechanisms for the k_4 step can be envisioned: the direct protonation of the nitrogen of the enamide ligand of **6a** by 2,6-dimethylaniline to regenerate the bisamide **1a** or the α-elimination of the enamine from **6a** to generate the imido intermediate. If **6a** α-eliminates enamine, in the presence of diphenylacetylene the resulting imido complex would be trapped to give metallacycle **3a**. When **6a** was heated to 45 °C in the presence of diphenylacetylene or 2,6-dimethylaniline, metallacycle **3a** and the bisamide **1a**, respectively, were formed at comparable rates over a 40-h period. This suggests that the α-elimination pathway is at least competitive with a mechanism involving direct amine exchange for the final step in the cycle.

Since neither the imido complex nor the metallacycle were observed in the ^1H NMR spectra during the course of the kinetic runs, the steady-state assumption was applied to the mechanism in Scheme III with respect to both intermediates, and the following rate law was derived (eq 19). This can be simplified if the

$$\frac{d[\text{enamine}]}{dt} = -\frac{d[\text{amine}]}{dt} = \frac{k_1k_2k_3[\text{alkyne}][Cp_2Zr(NHAr)_2]}{k_{-1}(k_{-2} + k_3[\text{amine}])} \quad (19)$$

assumption that $k_3[\text{amine}] > k_{-2}$ is made. This appears to be a valid assumption when aryl alkynes are used; however, as can be seen in Figure 4, it does not hold late in the reaction when [amine] is low and the plots of $[\text{amine}]^2/2$ vs time deviate from linearity. The simplified rate law is given in eq 20.

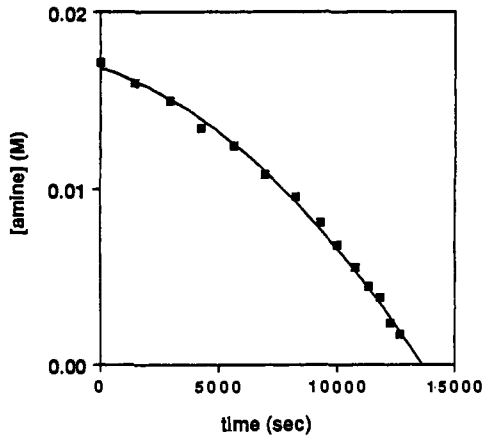

Figure 3. Plot of the concentration of amine vs time for kinetic run no. 4.

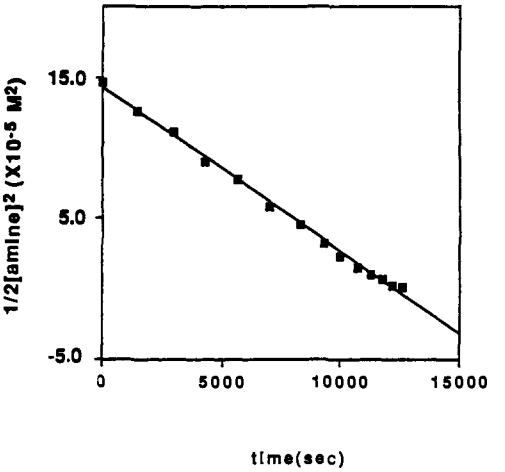

Figure 4. Plot of $^1/_2[\text{amine}]^2$ vs time for kinetic run no. 4.

$$-\frac{d[\text{amine}]}{dt} = \frac{k_1k_2[\text{alkyne}][Cp_2Zr(NHAr)_2]}{k_{-1}[\text{amine}]} \quad (20)$$

In the presence of at least a ten-fold excess of diphenylacetylene, its concentration and that of the catalyst were found to be constant (^1H NMR) through at least 3 half-lives. Under these conditions, the rate is predicted to be inverse first order with respect to the amine concentration (eq 21).

$$-\frac{d[\text{amine}]}{dt} = k_{obs}\left[\frac{1}{[\text{amine}]}\right] \quad (21)$$

The integrated form of this rate law is given in eq 22. Plots of [amine] vs time indicate that as time progresses the rate of the formation of enamine increases (Figure 3). This is consistent with the predicted inverse dependence on the amine concentration: as

$$\frac{1}{2}\left[[\text{amine}]_o^2 - [\text{amine}]^2\right] = k_1 \quad (22)$$

the amine is incorporated into the enamine there is less amine to inhibit the reaction through k_{-1}, and so the rate increases. A plot of $[\text{amine}]^2/2$ vs time yields a straight line, also in agreement with the predicted rate law (Figure 4). The initial concentrations of bisamide, diphenylacetylene, and 2,6-dimethylaniline along with the derived complex rate constant ratios k_1k_2/k_{-1} are listed in Table IV. In kinetic runs 1–4 the initial concentrations of the amine and the alkyne were held constant, and the concentration of the bisamide **3a** was varied from 3.57×10^{-4} to 5.60×10^{-3} M (Table IV). A plot of k_{obs} vs the concentration of the catalyst (Figure 5) clearly indicates the reaction is first order in the catalyst

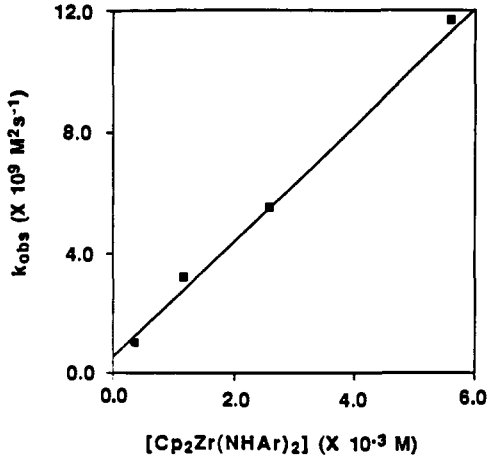

Figure 5. Plot of k_{obs} vs the concentration of catalyst.

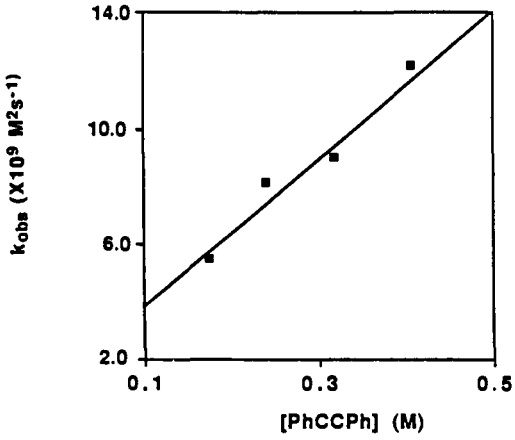

Figure 6. Plot of k_{obs} vs the concentration of alkyne.

3a. In kinetic runs 1, 5, 6, and 7 the initial concentration of the amine and catalyst are the same, while the concentration of the alkyne is varied from 0.164 to 0.405 M (Table IV). Plotting k_{obs} vs the alkyne concentration again yields a straight line indicating the reaction is first order in alkyne as shown in Figure 6. The rate constant ratios k_1k_2/k_{-1} can be derived for each kinetic run; we believe these are equal within experimental error of each other (Table IV).

Limitations of the Catalytic Formation of Enamines. Minor changes in the structure of bisamide can greatly affect the outcome of the catalytic reaction. We believe that the rate of α-elimination from bisamides **1** is controlled largely by the relief of steric strain in going to the imido complex $Cp_2Zr{=}NAr$, and thus, elimination of the smaller amine 4-*tert*-butylaniline is less favorable than elimination of the bulkier 2,6-dimethylaniline or *tert*-butylamine. We hoped to accelerate catalytic production of enamine by lowering the barrier to α-elimination using very large amide ligands. Heating a benzene solution of **1e** for 6 days with 4.0 equiv of diphenylacetylene at 140 °C resulted in no reaction. However, heating the metallacycle **3e** (made from the thermolysis of $Cp_2Zr(NHSi(CMe_3)Me_2)(CH_2CH_2CMe_3)$ with diphenylacetylene) with *tert*-butyldimethylsilylamine gave the bisamide **1e** and free diphenylacetylene *without* formation of the enamine which would be expected from the direct protonation of the metallacycle. It appears that steric hindrance can change the ratio of k_{-2}/k_3 and make protonation of the metallacycle relatively slow compared with cycloreversion.

Hydroamination of C–C Double Bonds. Attempts to hydroaminate olefins such as ethylene, allylbenzene, and norbornene with bisamides **1a** and **1d** and the corresponding amines at temperatures up to 160 °C were unsuccessful. If the azametallacyclobutenes are formed in these reactions, cycloreversion must be much faster than protonation as was observed with bisamide **1e** and metallacycle **3e**. However, when the more reactive C–C double bond of allene is utilized, hydroamination occurs readily at 95 °C providing the anti-Markovnikov product, the 2,6-dimethylphenylimine of acetone (eq 12).

Conclusion

We have shown that the imido intermediate $Cp_2Zr{=}NR$ exhibits a rich, controllable, and useful range of chemistry. The application of the bisamides $Cp_2Zr(NHR)_2$ and the alkyl amides $Cp_2Zr(NHR)(R')$ to the hydroamination of alkynes and allene provides a new method for the synthesis of enamines and imines. We have proposed a mechanism involving the intermediacy of the imido $Cp_2Zr{=}NR$ complex, azametallacyclobutenes, and the enamide amide **6a** which is supported by kinetic and stoichiometric experiments. Using the insights we have gained into this process, we hope to be able to develop methodology for the catalytic amination and hydroxylation of olefins.

Experimental Section

General Methods. Unless otherwise noted, all manipulations were carried out under an inert atmosphere in a Vacuum Atmospheres 553-2 drybox with attached M6-40-1H Dritrain or by using standard Schlenk or vacuum line techniques. Degassed solutions were frozen to −196 °C, evacuated under high vacuum, and thawed. This sequence was repeated three times in each case. Glass reaction vessels fitted with ground glass joints and Teflon stopcocks are referred to as bombs.

^1H NMR spectra were obtained on either the 250, 300, 400, or 500 MHz Fourier transform spectrometers at the University of California, Berkeley (UCB) NMR facility. The 250 and 300 MHz instruments were constructed by Mr. Rudi Nunlist and interfaced with either a Nicolet 1180 or 1280 computer. The 400 and 500 MHz instruments were commercial Bruker AM series spectrometers. ^1H NMR spectra were recorded relative to residual protiated solvent and are listed in Table V. ^{13}C NMR spectra were obtained at either 75.4 or 100.6 MHz on the 300 or 400 MHz instruments, respectively, and chemical shifts were recorded relative to the solvent resonance. The $^{13}C\{^1H\}$ NMR data are listed in Table VI. Chemical shifts are reported in units of parts per million downfield from tetramethylsilane, and all coupling constants are reported in Hz.

IR spectra were obtained on a Nicolet 510 FT-IR spectrometer. Mass spectroscopic (MS) analyses were obtained at the UCB mass spectrometry facility on AEI MS-12 and Kratos MS-50 mass spectrometers. Elemental analyses were obtained from the UCB Microanalytical Laboratory.

Sealed NMR tubes were prepared using Wilmad 505-PP and 504-PP tubes and were attached via Cajon adapters directly to Kontes vacuum stopcocks and degassed using freeze–pump–thaw cycles before flame sealing.[42] Known volume bulb vacuum transfers were accomplished with an MKS Baratron attached to a high vacuum line.

Unless otherwise specified, all reagents were purchased from commercial suppliers and used without further purification. 2,6-Dimethylaniline, 4-*tert*-butylaniline, and 2-methylaniline (Aldrich) were dried over sodium and distilled under vacuum. *tert*-Butylamine was refluxed over CaH_2 and vacuum transferred. Lithium amides were generated in situ by deprotonation of the corresponding amine with *n*-butyllithium in THF at room temperature.

Pentane and hexanes (UV grade, alkene free) were distilled from sodium benzophenone ketyl/tetraglyme under nitrogen. Benzene, toluene, ether, and THF were distilled from sodium benzophenone ketyl under nitrogen. Deuterated solvents for use in NMR experiments were dried as their protiated analogues but were vacuum transferred from the drying agent. Cp_2ZrMe_2,[24] $Cp_2Zr(Me)(Cl)$,[21,43] $Cp_2Zr(CH_2CH_2CMe_3)(Cl)$,[44] and $H_2NSi(CMe_3)Me_2$[45] were prepared by literature methods. Compounds **1a**, **1b**, **1c**, **1d**, **1e**, **2b**, **2c**, **2d**, and **2e** are reported elsewhere.[25]

$Cp_2Zr(NH(2,6\text{-}Me_2\text{-}C_6H_3))(Me)$ (2a). To a stirred solution of $Cp_2Zr(Me)(Cl)$ (373 mg, 1.37×10^{-3} mol) in 40 mL of THF was added $LiNH(2,6\text{-}Me_2C_6H_3)$ (175 mg, 1.38×10^{-3} mol) over a 5-min period at room temperature. The solution turned yellow after 15 min and was

(42) Bergman, R. G.; Buchanan, J. M.; McGhee, W. D.; Periana, R. A.; Seidler, P. F.; Trost, M. K.; Wenzel, T. T. In *Experimental Organometallic Chemistry: A Practicum in Synthesis and Characterization*; Wayda, A. L., Darensbourg, M. Y., Eds.; ACS Symposium Series 357; American Chemical Society: Washington, DC, 1987; p 227.
(43) Wailes, P. C.; Weigold, H.; Bell, A. P. *J. Organomet. Chem.* **1971**, *34*, 155.
(44) (a) Carr, D. B.; Schwartz, J. *J. Am. Chem. Soc.* **1979**, *101*, 3521. (b) Hart, D. W.; Schwartz, J. *J. Am. Chem. Soc.* **1974**, *96*, 5115.
(45) Bowser, J.; Nielson, R. H.; Wells, R. L. *Inorg. Chem.* **1978**, *17*, 1882.

Table V. ^{1}H NMR Data

δ (ppm)	multiplicity (J, Hz)	area	assignment	δ (ppm)	multiplicity (J, Hz)	area	assignment
			2a[a]				
0.21	s	3	CH_3	5.85	s	1	N-*H*
2.11	s	6	CH_3	6.94	t, 7.57	1	arom C-*H*
5.52	s	10	C_5H_5	7.10	d, 7.57	2	arom C-*H*
			3a[b]				
2.16	s	6	CH_3	6.75	m	4	arom C-*H*
6.12	s	10	C_5H_5	6.91	m	6	arom C-*H*
6.51	t, 7.44	1	arom C-*H*	7.10	t, 7.54	2	arom C-*H*
			3e[b]				
−0.02	s	6	CH_3	6.90	t, 7.70	2	arom C-*H*
0.62	s	9	$C(CH_3)_3$	7.04	d, 7.52	2	arom C-*H*
6.26	s	10	C_5H_5	7.13	tt, 1.81, 7.30	1	arom C-*H*
6.59	dd, 1.00, 8.10	2	arom C-*H*	7.19	t, 7.20	2	arom C-*H*
6.70	t, 7.34	1	arom C-*H*				
			4a[a]				
1.92	s	3	CH_3	6.47	m	3	arom C-*H*
2.23	s	6	CH_3	6.94	m	4	arom C-*H*
2.25	s	3	CH_3	7.11	m	4	arom C-*H*
5.85	s	10	C_5H_5				
			6a[c-e]				
2.13	s	3	CH_3	6.57	d, 7.63	2	C-*H*[e]
2.32	s	3	CH_3	6.79	m	5	C-*H*
2.42	s	3	CH_3	6.91	m	5	C-*H*
2.46	s	3	CH_3	7.02	d, 6.46	1	C-*H*
5.52	s	5	C_5H_5	7.11	m	2	C-*H*
6.32	s	1	N*H*[d]	7.25	t, 7.27	1	C-*H*
6.35	s	5	C_5H_5	7.36	d, 7.63	1	C-*H*
			7a[a]				
2.18	s	6	CH_3	7.01	m	3	arom C-*H*
4.20	s	1	N*H*	7.11	m	3	arom C-*H*
5.34	s	1	C*H*	7.51	m	2	arom C-*H*
6.85	m	5	arom C-*H*				
			8a[a]				
1.22	s	3	CH_3	6.92	t, 7.44	1	arom C-*H*
1.89	s	3	CH_3	7.01	d, 7.44	2	arom C-*H*
1.99	s	6	CH_3				

[a] C_6D_6, 25 °C. [b] THF-d_8, 25 °C. [c] CD_2Cl_2, −75 °C. [d] Assignment based on comparison of chemical shifts of other Zr-N*H*R moieties. [e] The resonances of the vinyl and aromatic C–H's could not be differentiated.

stirred for 20 h. The THF was removed under reduced pressure, and the remaining solid was taken up in 15 mL of toluene and filtered to remove the LiCl. The toluene solution was then concentrated to 4 mL in vacuo, layered with 2 mL of hexanes, and cooled to −30 °C. Yellow crystals were collected by decanting the solvent and washing the crystals with hexanes furnishing 251 mg (7.04×10^{-3} mol, 51% yield) of **2a**: IR (C_6H_6) 3311 (w), 2929, 2799, 2728, 2081, 1587, 1445, 1425, 1374, 1254, 1218, 1094, 910 cm^{-1}. Anal. Calcd for $C_{19}H_{23}NZr$: C, 63.99; H, 6.50; N, 3.93. Found: C, 63.85; H, 6.55; N, 3.88.

$C_{32}H_{29}NZr$ (3a). A bomb charged with **2a** (135 mg, 3.79×10^{-4} mol), diphenylacetylene (351 mg, 1.97×10^{-3} mol, 5.21 equiv), and 10 mL of benzene was degassed and heated at 85 °C. After 4 days at 85 °C the solution had become brown. The solvent was removed under reduced pressure, and the brown solid was dissolved in 4 mL of toluene, layered with an equal volume of hexanes and cooled to −30 °C. Large brown crystals were collected by filtration and washed with hexanes yielding 120 mg (2.63×10^{-4} mol, 70%) of **3a**: IR (C_6H_6) 1589 (w), 1434, 1415, 1293, 1271, 1238, 1102, 945, 801, 788, 766, 756, 731, 603 cm^{-1}; MS (EI) *m/e* 517 (M^+), 176 (base); UV–vis (toluene) λ_{max} = 300 nm (ϵ 2.2×10^4), λ = 361 nm (ϵ 8.1×10^3). Anal. Calcd for $C_{32}H_{29}NZr$: C, 74.08; H, 5.63; N, 2.70. Found: C, 73.87; H, 5.86; N, 2.73.

$C_{30}H_{35}SiNZr$ (3e). A glass bomb was charged with alkyl amide **2e** (499.6 mg, 1.14×10^{-3} mol), diphenylacetylene (204.1 mg, 1.15×10^{-3} mol), and 20 mL of benzene. The solution was degassed and heated at 110 °C for 2 days, turning dark brown after 2 h. The volatile materials were removed under reduced pressure, and the product was recrystallized from 7 mL of hexanes at −30 °C to give metallic purple flakes of the metallacycle (444.8 mg, 8.41×10^{-4} mol, 74%): IR (Nujol) 1588, 1506, 1439, 1252, 1094, 967, 824, 794 cm^{-1}. We were unable to obtain satisfactory elemental analysis on this compound.

$C_{34}H_{33}NZr$ (4a). The bisamide **1a** (175 mg, 3.81×10^{-4}) was put into a glass bomb along with di-*p*-tolylacetylene (236 mg, 1.14×10^{-3} mol, 3.3 equiv) and 10 mL of benzene. The solution was degassed and heated to 110 °C for 36 h during which time it turned green-brown. The volatile materials were removed under reduced pressure, and the remaining oil was taken up in ether and cooled to −30 °C. The white flakes that crystallized from solution were determined to be di-*p*-tolylacetylene by ^{1}H NMR spectrometry. The ether was removed under vacuum, and the remaining oil was dissolved in 3 mL of a toluene/hexanes mixture (6:1 ratio) and cooled to −30 °C. Crystals formed using this technique were collected by decanting the solvent and washing the crystals with cold hexanes providing 123 mg (2.26×10^{-4} mol, 59%): IR (Nujol) 1590, 1521, 1505, 1414, 1305, 1291, 1270, 1238, 1177, 1108, 1052, 1016, 944, 824, 797, 776, 726, 718, 651, 626, 594, 568, 535 cm^{-1}. We were unable to obtain crystals suitable for analysis.

$Cp_2Zr(N(2,6\text{-}Me_2\text{-}C_6H_3)CPhCHPh)(NH\text{-}2,6\text{-}Me_2\text{-}C_6H_3)$ (6a). To a solution of metallacycle **3a** (246.5 mg, 4.76×10^{-4} mol) in 5 mL of toluene was added 2,6-dimethylaniline (58.5 mg, 4.83×10^{-4} mol, 1.0 equiv) at 25 °C. The solution turned from brown to orange in 10 min and was stirred for an additional 20 min. The volatile materials were removed under reduced pressure, and the product was recrystallized from 2 mL of toluene layered with 4 mL of hexanes at −30 °C to give orange crystals of enamide **6a** (203.0 mg, 3.17×10^{-4} mol, 67%): IR (C_6H_6) 3311 (w), 3086, 1591, 1581, 1467, 1442, 1255, 1176, 1090, 819 cm^{-1}. Anal. Calcd for $C_{40}H_{40}N_2Zr$: C, 75.07; H, 6.30; N, 4.38. Found: C, 74.87; H, 6.25; N, 4.35.

$(2,6\text{-}Me_2\text{-}C_6H_3)NHCPhCHPh$ (7a). Bisamide **1a** (17.9 mg, 3.88×10^{-5} mol), diphenylacetylene (201.6 mg, 1.13×10^{-3} mol, 29.1 equiv), and 2,6-dimethylaniline (136.8 mg, 1.13×10^{-3} mol, 29.1 equiv) were dissolved in 25 mL of benzene, and the resulting solution was loaded into

Table VI. $^{13}C\{^1H\}$ NMR Data

δ (ppm)	assignment	δ (ppm)	assignment	δ (ppm)	assignment
			2a[b]		
18.92	*C*H$_3$	122.15	arom *C*-H	131.45	quat
20.35	*C*H$_3$	128.24	arom *C*-H	156.19	quat
110.56	*C*$_5$H$_5$				
			3a[a]		
21.59	*C*H$_3$	127.89	arom *C*-H	130.15	quat
112.53	*C*$_5$H$_5$	128.12	arom *C*-H	135.10	quat
120.93	arom *C*-H	128.25	arom *C*-H	149.20	quat
123.49	arom *C*-H	129.38	arom *C*-H	151.77	quat
126.84	quat	129.97	arom *C*-H	180.58	quat
127.17	arom *C*-H				
			3e[a]		
1.24	*C*H$_3$	124.43	quat	130.60	arom *C*-H
19.86	*C*(CH$_3$)$_3$	127.37	arom *C*-H	139.74	quat
28.07	C(*C*H$_3$)$_3$	127.90	arom *C*-H	146.94	quat
112.52	*C*$_5$H$_5$	128.31	arom *C*-H	169.81	quat
122.85	arom *C*-H	128.80	arom *C*-H		
			4a[b]		
20.73	*C*H$_3$	127.40	arom *C*-H	131.51	quat
20.81	*C*H$_3$	128.26	arom *C*-H	132.12	quat
21.21	*C*H$_3$	128.61	arom *C*-H	136.15	quat
111.25	*C*$_5$H$_5$	128.99	arom *C*-H	145.43	quat
120.56	arom *C*-H	129.12	arom *C*-H	151.06	quat
125.60	quat	131.20	quat	180.22	quat
			6a[d]		
20.07	*C*H$_3$	127.41	*C*-H	131.15	quat
21.81	*C*H$_3$	127.50	*C*-H	133.59	quat
21.97	*C*H$_3$	127.55	*C*-H	136.37	quat
111.20	*C*$_5$H$_5$	127.66	*C*-H	139.58	quat
112.63	*C*$_5$H$_5$	127.73	*C*-H	139.90	quat
116.19	*C*-H	127.93	*C*-H	154.96	quat
121.30	*C*-H	128.04	*C*-H	155.52	quat
123.25	*C*-H	128.18	*C*-H	157.04	quat
127.10	*C*-H	129.37	quat		
			7a[b]		
18.23	*C*H$_3$	128.55	*C*-H	135.20	quat
101.18	*C*-H	128.78	*C*-H	138.63	quat
124.28	*C*-H	128.84	*C*-H	138.99	quat
125.94	*C*-H	128.91	*C*-H	139.08	quat
128.09	*C*-H	129.83	*C*-H	143.54	quat
			8[b]		
17.69	*C*H$_3$	122.41	*C*H$_3$	149.41	quat
19.46	*C*H$_3$	125.49	quat	166.66	quat
26.90	*C*H$_3$	127.89	arom *C*-H		

[a] THF-d_8, 25 °C. [b] C_6D_6, 25 °C. [c] The resonance for the ipso carbon of the *i*-PrPh group could not be found in THF-d_8 or C_6D_6. [d] CD_2Cl_2 −25 °C: Due to the large number of carbons with similar chemical shifts we were unable to obtain a carbon spectrum between 25 and −95 °C in which resonances for all carbons were found. In the spectrum above one of the 2,6-dimethylphenyl rings is frozen and one of the phenyl groups is beginning to coalesce and has five resonances at this temperature. The enamide C–H could not be differentiated from the aromatic C–H's.

a glass bomb. The solution was degassed and heated at 120 °C for 13 days. The solvent was then removed under reduced pressure, and the product was crystallized from 5 mL of toluene layered with 2 mL of hexanes to give yellow crystals (203 mg, 6.78×10^{-4} mol, 60%): IR (C_6H_6) 3391, 3022, 2959, 1629, 1598, 1498, 1447, 1213, 771, 702, 697 cm^{-1}; MS (EI) *m/e* 299 (M^+), 208 (base). Anal. Calcd for $C_{22}H_{21}N$: C, 88.25; H, 7.07; N, 4.68. Found: C, 88.38; H, 7.09; N, 4.69.

Me_2C=N(2,6-Me_2-C_6H_3) from Allene and 2,6-Dimethylaniline. 2,6-Dimethylaniline (359 mg, 2.96×10^{-3} mol) and the bisamide **1a** (36.9 mg, 7.99×10^{-5} mol, 2.7 mol %) and 25 mL of C_6H_6 were loaded into a 1-L glass bomb and degassed, and 700 Torr of allene was added by vacuum transfer. The bomb was heated for 6 days at 90 °C at which time the volatile materials were removed under reduced pressure to yield a cloudy yellow oil. The oil was extracted into 20 mL of hexanes and filtered, and the solvent was removed under vacuum to provide 395 mg (2.45×10^{-3} mol, 83%) of the imine **8** judged pure by NMR: IR (neat) 2943 (br,s), 1694, 1667, 1594, 1470 (s), 1464, 1455, 1434, 1441, 1434, 1371, 1366, 1240, 1217, 1094, 1054, 846, 788, 752, 685, 575, 526, 507, 500 cm^{-1}.

Me_2C=N(2,6-Me_2-C_6H_3) from Acetone and 2,6-Dimethylaniline. 2,6-Dimethylaniline (2.10 g, 1.73×10^{-2} mol), dry 4-Å molecular sieves (10 g), and 30 mL of reagent grade acetone were loaded into a 1-L glass bomb, and the solution was degassed. The bomb was heated for 2 days at 85 °C at which time the solution was filtered, and the volatile materials were removed under reduced pressure to yield the imine as a yellow oil (2.58 g, 1.6×10^{-2} mol, 92%). The imine synthesized in this manner was identical to that prepared above by ^1H NMR spectrometry.

Structural Data for 3a. Isolation and Mounting. Brown prismatic crystals of compound **3a** were obtained by slow crystallization by diffusion of hexanes into toluene at −40 °C. Some of these crystals were mounted in thin-wall glass capillaries in a nitrogen-atmosphere glovebox and then flame sealed. Preliminary precession photographs indicated monoclinic Laue symmetry and yielded approximate cell dimensions.

The crystal used for data collection was then transferred to our Enraf-Nonius CAD-4 diffractometer and centered in the beam.[46] Auto-

(46) For a description of the X-ray diffraction and analysis protocols used, see: (a) Hersh, W. H.; Hollander, F. J.; Bergman, R. G. *J. Am. Chem. Soc.* **1983**, *105*, 5834. (b) Cromer, D. T.; Waber, J. T. *International Tables for X-ray Crystallography*; Kynoch Press: Birmingham, England, 1974; Vol. IV, Table 2.2B.

matic peak search and indexing procedures yielded the monoclinic reduced primitive cell. The final cell parameters and specific data collection parameters for this data set are given in Table I.

Structure Determination. The 7253 unique raw intensity data were converted to structure factor amplitudes and their esd's by correction for scan speed, background, and Lorentz and polarization effects. No correction for crystal decomposition was necessary. Inspection of the azimuthal scan data showed a variation $I_{min}/I_{max} = 0.96$ for the average curve. An empirical correction based on the observed variation was applied to the data. Inspection of the systematic absences indicated uniquely space group $P2_1/c$. Removal of systematically absent and redundant data left 6632 unique data in the final data set.

The structure was solved by Patterson methods and refined via standard least-squares and Fourier techniques. In a difference Fourier map calculated following the refinement of all non-hydrogen atoms with anisotropic thermal parameters, peaks were found corresponding to the positions of most of the hydrogen atoms. Hydrogen atoms were assigned idealized locations and values of B_{iso} approximately 1.25 times the B_{eqv} of the atoms to which they were attached. They were included in structure factor calculations but not refined. Before the final refinement cycles five reflections which apparently suffered from multiple diffraction were removed from the data set.

The final residuals for 614 variables refined against the 4660 data for which $F^2 > 3(F^2)$ were $R = 3.35\%$, wR = 4.13%, and GOF = 1.769. The R value for all 6627 data was 9.97%.

The quantity minimized by the least-squares program was $\sum w(|F_o| - |F_c|)^2$, where w is the weight of a given observation. The p-factor, used to reduce the weight of intense reflections, was set to 0.05 throughout the refinement. The analytical forms of the scattering factor tables for the neutral atoms were used, and all scattering factors were corrected for both the real and imaginary components of anomalous dispersion.[46b]

Inspection of the residuals ordered in ranges of $\sin(\theta/\lambda)$, $|F_o|$, and parity and value of the individual indexes showed no unusual features or trends. The largest peak in the final difference Fourier map had an electron density of 0.34 $e^-/Å^3$, and the lowest excursion was −0.45 $e^-/Å^3$. Both were located near the Zr atom.

The positional and thermal parameters of the non-hydrogen atoms are given in the tables. Anisotropic thermal parameters and the positions and thermal parameters and a listing of the values of F_o and F_c are included as supplementary material.

Structural Data for 7a. Isolation and Mounting. Pale yellow prismatic crystals of compound **7a** were obtained by slow crystallization from diffusion of hexanes into toluene at −30 °C. Some of these crystals were mounted in thin-wall glass capillaries and then flame sealed.

The crystal used for data collection was then transferred to our Enraf-Nonius CAD-4 diffractometer and centered in the beam. Automatic peak search and indexing procedures yielded the triclinic reduced primitive cell. The final cell parameters and specific data collection parameters for this data set are given in Table I.

Structure Determination. The 2203 unique raw intensity data were converted to structure factor amplitudes and their esd's by correction for scan speed, background, and Lorentz and polarization effects. No correction for crystal decomposition was necessary. Inspection of the azimuthal scan data showed a variation of $I_{min}/I_{max} = 0.84$ for the average curve. An empirical correction based on the observed variation was applied to the data.

The structure was solved via SHELXS and refined via standard least-squares and Fourier techniques. All atoms were refined with isotropic thermal parameters. The final residuals for 93 variables refined against the 1577 data for which $F^2 > 3\sigma(F^2)$ were $R = 10.3\%$, wR = 13.1%, and GOF = 4.73. The R value for all 2203 data was 13.1%. The final difference Fourier map showed maximum excursions of +0.66 and −0.36 e/Å^3.

Kinetic Studies of the Catalytic Formation of Enamines. ^{1}H NMR spectrometry was used to study the catalytic formation of enamine **7a** from 2,6-dimethylaniline and diphenylacetylene using bisamide **1a** as the catalyst and p-dimethoxybenzene as the internal standard. The disappearance of amine was monitored as the reaction progressed at 95 °C.

Two stock solutions were prepared. Stock solution no. 1 contained 38.3 mg (8.29×10^{-5} mol, 1.66×10^{-2} M) of bisamide **1a** and 58.6 mg (4.25×10^{-4} mol, 8.50×10^{-2} M) of p-dimethoxybenzene internal standard in 5.00 mL of C_6D_6 in a volumetric flask. Stock solution no. 2 contained 51.5 mg (4.26×10^{-4} mol, 8.52×10^{-2} M) of 2,6-dimethylaniline in 5.00 mL of C_6D_6 in a volumetric flask. These solutions were stored in the drybox at −30 °C between uses.

In a typical run a 1.00 ± 0.01 mL volumetric flask was charged with 30.0 mg (1.68×10^{-4} mol) of diphenylacetylene, 0.20 ± 0.005 mL of stock solution no. 1, 0.20 ± 0.005 mL of stock solution no. 2, and C_6D_6 was added to bring the total volume to 1.00 mL. Based on the weights used the calculated concentrations of the reactants were 1.70×10^{-2} M 2,6-dimethylaniline, 1.70×10^{-2} M p-dimethoxybenzene, 1.70×10^{-1} M diphenylacetylene, and 3.22×10^{-3} M bisamide **1a**. The solution was transferred to a 7″ NMR tube, degassed by two freeze–pump–thaw cycles, and flame sealed. The sample was allowed to equilibrate in the magnet of a 300 MHz Nicolet NMR spectrometer for 3 min, and then a one-pulse ^{1}H NMR spectrum was taken. After 3 min another one-pulse ^{1}H NMR spectrum was taken. Both scans were separately exponentially multiplied, Fourier transformed, and plotted with integrals. The concentration of amine was then determined by integration against the internal standard for each one-pulse ^{1}H NMR spectrum, and then the results from the two spectra were averaged and taken as the time zero point. The concentrations of the reactants were determined by this method to be 1.72×10^{-2} M 2,6-dimethylaniline, 2.67×10^{-3} M bisamide **1a**, and 1.61×10^{-1} M diphenylacetylene. In general the integrated concentrations agreed well with the calculated concentrations. However, the integrated catalyst concentration was consistently low, presumably due to a small amount of water which reacted with the bisamide **1a** as observed by ^{1}H NMR spectrometry. This impurity did not change nor did it appear to affect the measured rate during the experiment. The sample was then heated at 95 °C, and the procedure described above was used to take spectra at time intervals of 30 min at the beginning of the run and 15 min between the first half-life and the end of the run. The data were then analyzed according to eq 22. A typical plot of $^1/_2$[amine]^2 vs time from which the rate constant k_{obs} was determined is shown in Figure 4. The rate constant data are presented in Table IV.

Reaction of 3a with Di-p-tolylacetylene. An NMR tube was charged with metallacycle **3a** (7.7 mg, 1.49×10^{-5} mol), di-p-tolylacetylene (15.3 mg, 7.43×10^{-5} mol, 5.0 equiv), and 0.7 mL of C_6D_6. The solution was degassed, and the NMR tube was flame sealed. The solution was heated at 45 °C and monitored by ^{1}H NMR spectrometry. The formation of metallacycle **4a** was observed, and an equilibrium was reached between **3a** and **4a** and the diarylalkynes after 4 days.

Reaction of 3a with Excess 2,6-Dimethylaniline. Metallacycle **3a** (12.9 mg, 2.49×10^{-5} mol) and p-dimethoxybenzene (3.2 mg, 2.32×10^{-5} mol) were dissolved in 0.7 mL of C_6D_6. An NMR spectrum was taken, and the concentration of the metallacycle was determined by integration against p-dimethoxybenzene. Then 2,6-dimethylaniline (6.4 mg, 5.29×10^{-5} mol, 2.1 equiv) was added to the solution. The solution was degassed, and the NMR tube was flame sealed. The reaction was heated at 45 °C for 40 h and another NMR spectrum was taken to determine the concentration of bisamide **1a** and enamine **7a** by integration against p-dimethoxybenzene. The yields of enamine and bisamide were determined to be 97% by this method.

Reaction of 6a with Di-p-tolylacetylene. An NMR tube was charged with enamide **6a** (7.4 mg, 1.12×10^{-5} mol), di-p-tolylacetylene (12.0 mg, 5.82×10^{-5} mol, 5.2 equiv), and 0.7 mL of C_6D_6. The solution was degassed, and the NMR tube was flame sealed. The solution was heated at 45 °C, and the reaction was monitored by ^{1}H NMR spectrometry. Formation of metallacycle **4a** and enamine **7a** were observed to be complete after 40 h. In a separate experiment the yield of metallacycle **4a** was determined as follows. Enamide **6a** (14.1 mg, 2.2×10^{-5} mol), di-p-tolylacetylene (6.8 mg, 3.30×10^{-5} mol), and p-dimethoxybenzene (3.0 mg, 2.17×10^{-5} mol) were dissolved in 0.7 mL of C_6D_6 and put in an NMR tube. The solution was degassed, and the NMR tube was flame sealed. The concentration of enamide **6a** was determined by integration of the ^{1}H NMR spectrum against p-dimethoxybenzene. The sample was then heated at 95 °C for 18 h, and the final yield of metallacycle **4a** (>95%) and enamine **7a** (87%) were determined by integration against p-dimethoxybenzene.

Reaction of 6a with 2,6-Dimethylaniline. An NMR tube was charged with enamide **6a** (7.4 mg, 11.2×10^{-5} mol), 2,6-dimethylaniline (7.0 mg, 5.78×10^{-5} mol, 5.2 equiv), and 0.7 mL of C_6D_6. The solution was degassed, and the NMR tube was flame sealed. The solution was heated at 45 °C, and the formation of bisamide **1a** and the enamine **7a** were observed to be complete by NMR spectroscopy after 40 h. In a separate experiment the yield of bisamide **1a** and enamine **7a** were determined by ^{1}H NMR spectroscopy. Enamide (15.4 mg, 2.41×10^{-5} mol), 2,6-dimethylaniline (4.4 mg, 3.64×10^{-5} mol), and p-dimethoxybenzene (3.3 mg, 2.39×10^{-5} mol) were dissolved in 0.7 mL of C_6D_6 and put in a NMR tube. The solution was degassed, and the NMR tube was flame sealed. The initial concentration of enamide **6a** was determined by integration against p-dimethoxybenzene. The sample was then heated at 110 °C for 1 h, and the concentration of the product, bisamide **1a**, was determined by integration against p-dimethoxybenzene. In this way the yield of bisamide **1a** and enamine **7a** were determined to be greater than 97% each.

Reaction of 1e with PhCCPh. An NMR tube was charged with bisamide **1e** (11.5 mg, 2.38×10^{-5} mol), diphenylacetylene (17.0 mg, 9.55×10^{-5} mol, 4.0 equiv), and 0.7 mL of C_6D_6. The solution was degassed, and the NMR tube was flame sealed. The reaction was heated at 140

°C and monitored by ^{1}H NMR spectroscopy. No reaction was observed after 6 days.

Reaction 3e with $H_2NSi(CMe_3)Me_2$. An NMR tube was charged with metallacycle **3e** (7.0 mg, 1.32×10^{-5} mol), $H_2NSi(CMe_3)Me_2$ (3.8 mg, 2.90×10^{-5} mol, 2.2 equiv), and 0.7 mL of C_6D_6. The solution was degassed, and the NMR tube was flame sealed. The solution was heated at 95 °C, and the reaction was monitored by ^{1}H NMR spectrometry. After 4 days the conversion of metallacycle **3e** to diphenylacetylene and bisamide **1e** was observed to be complete with no other products formed. The reaction was also found to proceed at 45 °C, requiring several weeks for completion.

General Procedure for the Determination of Catalytic Turnover Rates. An NMR tube was charged with alkyne (2×10^{-4} mol), amine (2×10^{-4} mol), the catalyst (8×10^{-6}, 3 mol %), ferrocene internal standard, and 0.7 mL of C_6D_6. The solution was degassed, and the NMR tube was flame sealed. The reaction was heated at 110 °C and monitored by ^{1}H NMR spectrometry. The concentration of product was determined by integration against the internal standard ferrocene. In the cases where both imine and enamine were observed the product concentration was taken to be the sum of the imine and enamine concentrations.

Isomerization of 7a with I_2. An NMR tube was charged with enamine **7a** (10.6 mg, 3.54×10^{-5} mol), iodine (0.3 mg, 1.18×10^{-6} mol, 0.03 equiv), and 0.7 mL of C_6D_6. The tube was placed in room light for 1 h, and then a ^{1}H NMR spectrum was taken which indicated complete conversion to imine had taken place.

Acknowledgment. We are grateful for financial support of this work from the National Institutes of Health (Grant No. GM25457). We would like to thank Dr. F. J. Hollander, Director of the U.C. Berkeley X-ray Diffraction Facility (CHEXRAY), for solving the structures of **3a** and **7a**.

Registry No. 1a, 117939-64-7; **1b**, 138313-32-3; **1c**, 138313-33-4; **1d**, 117939-63-6; **1e**, 138313-34-5; **2a**, 117939-53-4; **2b**, 117939-51-2; **2c**, 138313-35-6; **2d**, 117939-52-3; **2e**, 138333-46-7; **3a**, 117939-60-3; **3e**, 138313-36-7; **4a**, 138313-37-8; **5a**, 138313-38-9; **6a**, 138313-39-0; **7a**, 138313-30-1; **8a**, 138313-31-2; **10**, 138313-40-3; $Cp_2Zr(Me)(Cl)$, 1291-45-8; $LiNH(2,6\text{-}Me_2C_6H_3)$, 111749-95-2; PhC≡CPh, 501-65-5; *p*-Tol-C≡C-Tol-*p*, 2789-88-0; $(2,6\text{-}Me_2C_6H_3)NH_2$, 87-62-7; $CH_2{=}C{=}CH_2$, 463-49-0; $Me_2C{=}N(2,6\text{-}Me_2C_6H_3)$, 85384-97-0; $H_2NSi(CMe_3)Me_2$, 41879-37-2; acetone, 67-64-1.

Supplementary Material Available: Tables of distances, angles, and *x*, *y*, *z* coordinates from the structure determinations of complexes **3a** and **7a** (10 pages). Ordering information is given on any current masthead page.

Photochemical Substitution Reactions of $[CpFe(CO)_2]_2$ (Cp = η^5-C_5H_5) in Hydrocarbon and Tetrahydrofuran Solution at Room Temperature: A Mechanistic Study with Time-Resolved Infrared Spectroscopy

Andrew J. Dixon, Michael W. George, Catherine Hughes, Martyn Poliakoff,* and James J. Turner*

Contribution from the Department of Chemistry, University of Nottingham, Nottingham, England NG7 2RD. *Received August 7, 1991*

Abstract: Microsecond and nanosecond time-resolved IR spectroscopy (TRIR) have been used to investigate both the kinetics and the nature of the intermediates in the photochemical substitution reactions of $[CpFe(CO)_2]_2$ (Cp = η^5-C_5H_5) with THF and $P(OR)_3$ (R = Me, Et, and ^{i}Pr) in cyclohexane and *n*-heptane solutions at 25 °C. An important feature of these experiments has been the use of both UV and visible photolysis wavelengths to distinguish between processes involving photoejection of CO, which principally occurs on UV irradiation, and homolysis of the Fe–Fe bond, which is promoted by both UV and visible light. TRIR signals from the depletion of $[CpFe(CO)_2]_2$ with 308-nm photolysis are used to determine the branching ratio (0.9:1) between homolysis of the Fe–Fe bond and photoejection of CO. These data then permit the evaluation of the IR extinction coefficient of the antisymmetric ν(C–O) band of the Fp radical, $CpFe(CO)_2$, and hence the rate constant for dimerization of Fp. High-resolution microsecond TRIR based on a continuously tunable IR diode laser calibrated by FTIR is used to show that, contrary to previous work, there is no significant difference in wavenumber of the ν(C–O) band of the Fp radical between microsecond and picosecond TRIR experiments. UV photolysis of $[CpFe(CO)_2]_2$ in the presence of THF provides TRIR evidence for the formation of a previously unknown species, $Cp_2Fe_2(CO)_3(THF)$, the formation of which involves neither Fp nor $Cp_2Fe_2(\mu\text{-}CO)_3$ and may well occur via a very short-lived and so far undetected precursor to $Cp_2Fe_2(\mu\text{-}CO)_3$. TRIR experiments on the reaction of $[CpFe(CO)_2]_2$ with $P(OMe)_3$ reveal a very rapid substitution of one CO group in the Fp radical by $P(OMe)_3$ followed by dimerization of $CpFe(CO)P(OMe)_3$ to form $[CpFe(CO)P(OMe)_3]_2$. Similar results were obtained with $P(OEt)_3$ and $P(O^iPr)_3$, although in these cases the $[CpFe(CO)P(OR)_3]_2$ compounds are labile and had not previously been detected. It is suggested that an IR band of an intermediate in these reactions, previously attributed to $CpFe(CO)_2(\mu\text{-}CO)CpFe(CO)P(O^iPr)_3$, is in fact due to $[CpFe(CO)P(O^iPr)_3]_2$. An overall scheme is given for the reactions, in which all of steps can be explained on the basis of three intermediates, $Cp_2Fe_2(\mu\text{-}CO)_3$, $CpFe(CO)_2$, and $CpFe(CO)P(OR)_3$; rate constants have been evaluated for most of the steps.

Introduction

The dinuclear iron complex, $[CpFe(CO)_2]_2$ (Cp = η^5-C_5H_5), has been the subject of chemical interest for many years, yet its behavior continues to yield surprises. Initial studies[1] focused on the solvent-dependent equilibrium between cis and trans isomers, **1** and **2**, and NMR spectroscopy was used to unravel the dynamics of the interconversion between these isomers,[2] one of the first examples of fluxionality in polynuclear organometallics. More recently, workers have concentrated on the rich photochemistry

(1) Manning, A. R. *J. Chem. Soc. A* **1968**, 1319; McArdle, P. A.; Manning, A. R. *J. Chem. Soc. A* **1969**, 1948.

(2) Bullitt, J. G.; Cotton, F. A.; Marks, T. J. *J. Am. Chem. Soc.* **1970**, *92*, 2155. Gansow, O. A.; Burke, A. R.; Vernon, W. D. *J. Am. Chem. Soc.* **1972**, *94*, 2550; **1976**, *98*, 5817.

0002-7863/92/1514-1719$03.00/0 © 1992 American Chemical Society